




Article

# Nexus between Energy Usability, Economic Indicators and Environmental Sustainability in Four ASEAN Countries: A Non-Linear Autoregressive Exogenous Neural Network Modelling Approach

Siti Indati Mustapa <sup>1</sup>, Freida Ozavize Ayodele <sup>2</sup>, Bamidele Victor Ayodele <sup>1,\*</sup>  
and Norsyahida Mohammad <sup>1</sup>

<sup>1</sup> Institute of Energy Policy and Research, Universiti Tenaga Nasional, Jalan Ikram-Uniten, Kajang 43000, Malaysia; indati@uniten.edu.my (S.I.M.); norsyahida.mohammad@uniten.edu.my (N.M.)

<sup>2</sup> Department of Accounting and Finance, UCSI University Kuala Lumpur, 1 Jalan Menara Gading, Taman Connaught, Cheras Kuala Lumpur 56000, Malaysia; freida.ayodele@yahoo.ca

\* Correspondence: ayodele.victor@uniten.edu.my

Received: 27 August 2020; Accepted: 3 October 2020; Published: 25 November 2020



**Abstract:** This study investigates the use of a non-linear autoregressive exogenous neural network (NARX) model to investigate the nexus between energy usability, economic indicators, and carbon dioxide (CO<sub>2</sub>) emissions in four Association of South East Asian Nations (ASEAN), namely Malaysia, Thailand, Indonesia, and the Philippines. Optimized NARX model architectures of 5-29-1, 5-19-1, 5-17-1, 5-13-1 representing the input nodes, hidden neurons and the output units were obtained from the series of models configured. Based on the relationship between the input variables, CO<sub>2</sub> emissions were predicted with a high correlation coefficient (R) > 0.9. and low mean square errors (MSE) of  $3.92 \times 10^{-21}$ ,  $4.15 \times 10^{-23}$ ,  $2.02 \times 10^{-19}$ ,  $1.32 \times 10^{-20}$  for Malaysia, Thailand, Indonesia, and the Philippines, respectively. Coal consumption has the highest level of influence on CO<sub>2</sub> emissions in the four ASEAN countries based on the sensitivity analysis. These findings suggest that government policies in the four ASEAN countries should be more intensified on strategies to reduce CO<sub>2</sub> emissions in relationship with the energy and economic indicators.

**Keywords:** ASEAN; CO<sub>2</sub> emissions; energy consumption; economic indicator; gross domestic product; NARX neural network

## 1. Introduction

In the past three decades, there has been rapid urbanization and industrialization among the Association of Southeast Asian Nations (ASEAN), which invariably has translated to economic growths, and high energy demand and consumption [1]. The increasing energy demand amongst the ASEAN countries is often met with energy derived from fossil sources most especially coal, natural gas, and oil [1,2]. The share of coal in the energy mix of ASEAN has been on the rise and has been projected to continue to increase in a long time [3,4]. Recent energy outlook by the international energy agency revealed that the rising fuel demands among Southeast Asian countries have surpassed the regional production hence, the possibility of becoming a net importer of fuel [5]. Although, the high energy demand is seen as the powerhouse that drives industrial and economic activities within the region, and it often comes with the cost of high carbon dioxide (CO<sub>2</sub>) emissions [6]. As shown in Figure 1, the increase in economic indicators and energy demand also translated into energy-related CO<sub>2</sub> emissions. To this effect, several energy economists have investigated the relationship between CO<sub>2</sub> emissions, economic growth and energy consumption, as summarized in Table 1. Proper understanding

of this relationship would help in finding lasting solutions to the age-long dilemma of sustainable economic growth and environmental pollution.

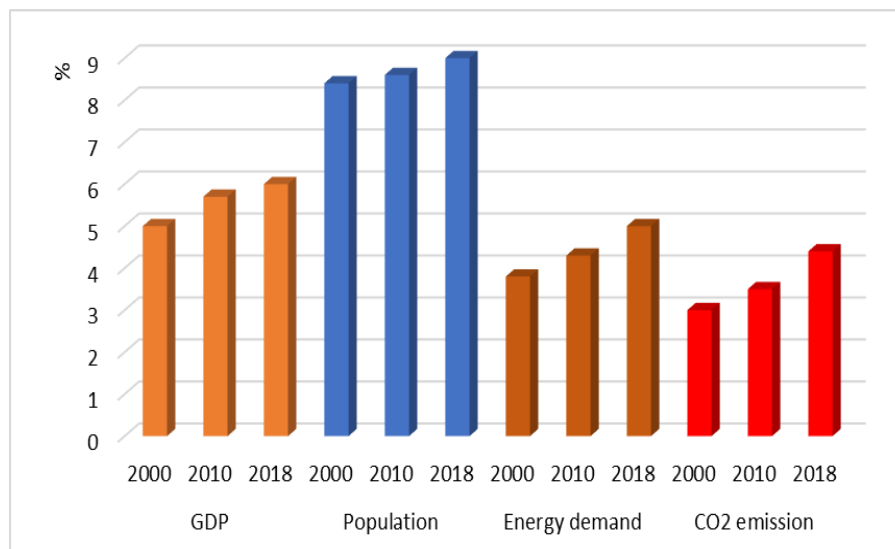


**Figure 1.** Share of Southeast Asia in global economic indicators, energy consumption and CO<sub>2</sub> emissions [5].

In the last one-decade various modelling techniques have been employed to investigate the causal relationship between CO<sub>2</sub> emissions, economic indicators, and energy consumption in various countries [7–10]. Modelling techniques, such as panel quantile regression approach, Simultaneous Equation Modelling, system of simultaneous equations using seemingly unrelated regression, and Cointegration-Vector Error Correction Modelling have been widely applied. Zhu et al. [11] and Heidari et al. [12] employed panel quantile regression model to investigate the effect of foreign direct investment (FDI), economic growth, and energy consumption on CO<sub>2</sub> emissions in Malaysia, Philippines, Indonesia, Malaysia, Singapore, and Malaysia. The study revealed that FDI, economic growth, and energy consumption have a heterogeneous effect on CO<sub>2</sub> emissions. However, the level of importance of the input variables, as well as the prediction of the CO<sub>2</sub> emissions, based on the variables, could not be ascertained using the panel quantile regression model. In a recent study, Salman et al. [13] also employed panel quantile regression for modeling the impact of export and import on carbon emissions in seven ASEAN countries namely Brunei, Indonesia, Malaysia, Philippines, Singapore, Thailand, and Vietnam. Using datasets between 1990–2017, the study revealed that CO<sub>2</sub> emissions in the seven ASEAN countries were significantly influenced by export and import. Besides export and import, the authors reported that CO<sub>2</sub> emissions increased by population size and energy intensity. However, the extent of influence and the level of importance of these variables were not reported. Also, the technique could not predict CO<sub>2</sub> emissions based on the non-linear relationship between the variables.

Beside panel quantile regression, other modelling techniques that have been employed in investigating relationship between CO<sub>2</sub> emissions, economic indicator, and energy consumption include Cointegration and Vector Error Correction Model [14], Auto-Regressive Integrated Moving Average (ARIMA) and Simple Exponential Smoothing Models [15], Autoregressive Distributive Lag (ARDL) model [16], Linear regression [17], Backpropagation neural network [17], non-linear dynamic neural network [17], and Simultaneous Equation Models [18]. These techniques were effective in explaining the causal relationship between CO<sub>2</sub> emissions and the various input variables investigated. However, one major shortcoming of these techniques is their inability to accurately predict CO<sub>2</sub> emissions based on the various input variables and their level of importance on the prediction, due to the non-linear relationship that exists between them. This shortcoming can be overcome

using the nonlinear autoregressive networks with exogenous input (NARX) [17]. The NARX model is a time series recurrent dynamic feedback neural networks that have the capability to model the interrelation between input and output variable for prediction purposes [19]. Moreover, the level of importance of these variables could also be determined using the vector weights that connect the input variables with the output [20]. Xu et al. [17] employed NARX technique to model the prediction of CO<sub>2</sub> emissions peak in China. Using datasets from 1978–2016, the study revealed that the NARX model was robust in predicting the CO<sub>2</sub> emissions in China with GDP having the highest level of influence based on the sensitivity analysis. To the best of the authors' knowledge, the use of NARX model for predictive modeling and to investigate the nonlinear relationship between economic indicators, energy consumptions and CO<sub>2</sub> emissions in ASEAN countries such as Malaysia, Thailand, Indonesia and the Philippines have not reported in the literature. This study is aimed at employing the NARX techniques for modelling the prediction of CO<sub>2</sub> emissions in Malaysia, Thailand, Indonesia and Philippines based on the nonlinear relationship that exist between them and to determine the level of importance of the prediction.

**Table 1.** Summary of literature on modelling of CO<sub>2</sub> emissions.

Countries Investigated	Methods	Variables	Reference
ASEAN (Malaysia, Thailand, Indonesia and the Philippines)	Autoregressive Exogenous Neural Network Modeling	Energy Consumption per capita, Population, GDP per capita	This study
ASEAN (Brunei, Indonesia, Malaysia, Philippines, Singapore, Thailand, Vietnam)	Panel quantile regression approach	Export and Import	[13]
Indonesia	Cointegration and Vector Error Correction Model	Energy Consumption, GDP, House Expenditure	[14]
Asian countries (Japan, Bangladesh, China, Pakistan, India, Sri Lanka, Iran, Singapore, and Nepal)	Auto-Regressive Integrated Moving Average (ARIMA) and Simple Exponential Smoothing Models	Heat and electricity, manufacturing industries, residential and commercial buildings, transport	[15]
Asia countries	Autoregressive Distributive Lag model.	Fossil fuel, FDI, GDP	[16]
China	Linear regression, Backpropagation neural network, non-linear dynamic neural network	GDP, total population, urbanization rate, total energy consumption, percentage of coal consumption, percentage of non-fossil consumption	[17]
Mediterranean countries	System of simultaneous equations using seemingly unrelated regression.	Research and Development Stocks, GDP.	[18]
Croatia	Environmental Kuznets Curve (EKC) model	Electricity Consumption, GDP	[18]
ASEAN (Malaysia, Indonesia, Philippines, Singapore, and Thailand)	Panel quantile regression model	Foreign Direct Investment, GDP, Energy Consumption	[11]
ASEAN (Malaysia, Indonesia, Philippines, Singapore, and Thailand)	Panel smooth transition regression model	Energy Consumption and GDP	[12]
India	Directed acyclic graphs	Energy Consumption, GDP, fixed capita formation, and Trade openness	[21]
Middle East, North Africa and Sub-Sahara Africa	Simultaneous Equation Models	Foreign direct investment,	[22]
China	System Dynamic Modelling	Energy Consumptions	[23]
Russia	Environmental Kuznets Curve (EKC) model	Energy Consumptions and GDP	[24]
India	System Dynamic Modelling	Energy Consumption and GDP	[25]
Turkey	autoregressive distributed lag bounds testing approach of cointegration	Energy consumption and economic indicator	[26]

## 2. Materials and Methods

### 2.1. Data Description

The variables used in this study for the NARX modelling were carefully selected based on previous literature summarized in Table 1. The CO<sub>2</sub> emissions as a function of kg per \$US of GDP, energy consumption per capita measured in kWh, GDP per capita (current \$US), population, oil consumption, coal consumption, were annual data from 1965–2018 obtained from World Bank Open database and British Petroleum energy database. The CO<sub>2</sub> emission (kg per 2010 \$US of GDP) represents the CO<sub>2</sub> emissions from industrial and human activities in the utilization of fossil fuel. The energy consumption per capita, which is one of the fundamental markers of economic development of any country, explains energy utilization by an individual per year. The causal relationship between energy consumption, CO<sub>2</sub> emissions and economic growth has been investigated by several authors using various modelling techniques as shown in Table 1. The annual coal consumption is the amount of coal required for electricity generation. The rapid industrialization of the four ASIAN countries requires high energy demand which heavily dependent on coal. Liu et al. [27] employed coal consumption as one of the variables in the scenario analysis of energy consumption and CO<sub>2</sub> emission in China using system dynamic model. Similarly, Chandran Govindaraju and Tang [28] also investigated the dynamic link between CO<sub>2</sub> emissions, coal consumption and economic growth in China and India. Oil consumption is the amount of crude oil utilized for refining purposes. There has been a steady increase in oil consumption in the four ASEAN countries over the years. The GDP per capita is an indicator of a country's economic growth as a function of the population. Over the years, the GDP per capita of the four ASEAN countries has increased steadily. This could be attributed to the rapid industrialization and economic growth of the region.

### 2.2. The NARX Neural Network Modelling

Artificial Neural Networks are biological system inspired learning models comprised of inbuilt algorithms with a number of interlinked neurons between the input and the output [29]. The network usually receives input signals which are transformed to output signals. The NARX is a time series feedback artificial neural networks represented in Equation (1) [30]. It comprises interconnected feedback synaptic and delays that provides a flow of signals between the neurons [31]. The major advantage of the NARX as a robust time-series modeling technique is the significance of the delay that supply the precise historical information of a set of data at the current moment and the feedback loop that help to filter the historical data thereby allowing for the prediction of more accurate output [32]. The model architecture of the NARX neural network is depicted in Figure 2. It consists of the input, hidden and output layers connected by artificial neurons. The artificial neurons execute certain actions on the input signals as shown in Equation (2). In Equation (2), the hidden nodes are estimated in terms of the weights of the paths associated with the input nodes and the bias path which is a component of the back-propagation algorithm [33]. The configuration makes use of the past and present values of  $u(t)$  as well as the actual past values of  $y(t)$  for the prediction of  $y(t + 1)$ . The multilayer perceptron topology which is a feedforward backpropagation network is often adopted in the training of the NARX [34]. The training entails the adjustment of the weights in such a manner that the errors between the actual and the predicted values are minimized [35]. These errors are usually measured as mean square error (MSE) defined in Equation (2) [36]. The robustness of the NARX predictive models is measured using the coefficient of correlation (R) represented in Equation (3). The model development was performed using the Neural Network toolbox in MATLAB version 2019 a (MathWorks Inc.),

$$y(t) = f(y(t-1), y(t-2), \dots, y(t-n_y), u(t-2), \dots, u(t-d_u)) \quad (1)$$

where  $y(t)$  = depicts the output of the NARX model and  $u(t)$  depicts the input of the NARX model.

$$MSE = \frac{1}{n} \sum_{i=1}^n (y_i - \hat{y}_i)^2 \tag{2}$$

$$R = \frac{n \sum y_i \hat{y}_i - (\sum y_i)(\sum \hat{y}_i)}{\sqrt{(n \sum y_i^2 - (\sum y_i)^2)(n \sum \hat{y}_i^2 - (\sum \hat{y}_i)^2)}} \tag{3}$$

where  $n$ ,  $y_i$ ,  $\hat{y}_i$ , are the number of observed variables, the observed outputs, and the predicted output, respectively.

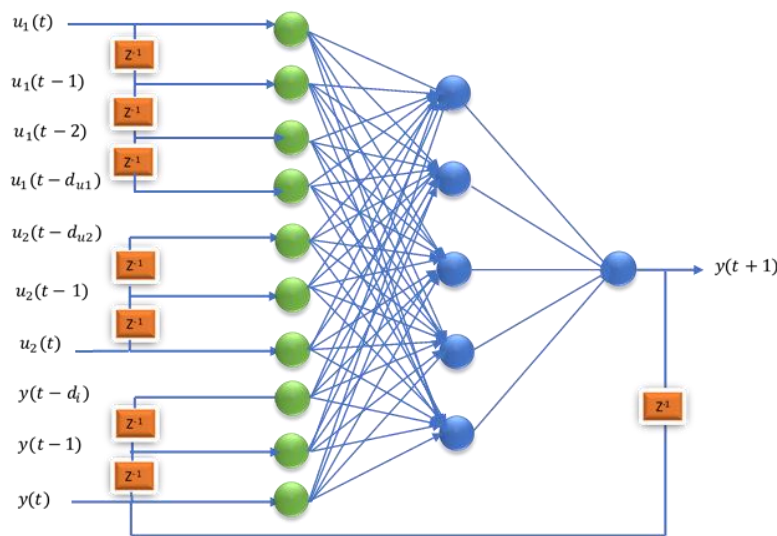


Figure 2. The model architecture of the NARX neural network.

In Equation (1) each of the successive output signals ( $y(t)$ ) is regressed on the preceding value of the ( $y(t)$ ) and the values of an exogenous input signal as shown in Equation (4).

$$\vartheta = \sum_k w_k x_k + b \tag{4}$$

where  $\vartheta$ ,  $w_k$ ,  $x_k$ ,  $b$ ,  $\theta$  are the neurons' output, the weight factor,  $k$ th input, the activation function and the bias. The sigmoid activation function represented in Equation (5) is often employed in predictive modeling due to its smoothen effect:

$$\theta = \frac{1}{1 + \exp^{-\vartheta}} \tag{5}$$

### 2.3. Sensitivity Analysis of the Input Variables

The sensitivity analysis to determine the level importance ( $\rho_{iz}$ ). of the input variables on the CO<sub>2</sub> emission per capita was determined using modified Garson's algorithm represented in Equation (6) [33,37]. The algorithm involves the partitioning of the connected weights of the hidden-output neurons within the NARX network into elements associated with each input neurons. The relative predictive importance of the input variables is revealed by the connection weights in the paths of each of the input nodes the corresponding output nodes [33],

$$\rho_{iz} = \frac{\sum_{k=1}^i |\omega_{ik} v_{jz}| / \sum_{x=1}^i |\omega_{xj}|}{\sum_{i=1}^n \sum_{k=1}^i |\omega_{ik} v_{jz}| / \sum_{x=1}^i |\omega_{xj}|} \tag{6}$$

where  $\omega_{ik}$ , depicts the weight between  $i$ th input and  $j$ th hidden unit;  $v_{jz}$  signifies the weight between the  $j$ th hidden unit and the  $z$ th output while  $x$  is the number of hidden neurons,  $\omega_{ik}$  is the weight of the  $x$ th input and  $j$ th hidden unit,  $n$  is the number of input neurons.

### 3. Results and Discussion

#### 3.1. Optimization of the Hidden Neurons

Optimization of the hidden neurons was performed to determine the number of hidden neurons that will minimize the MSE in the NARX neural network architecture. The hidden neurons were varied from 1 to 29 using different delays ranges from 1 to 15 (See Tables A1–A4 in the Appendix A for detail of the optimization). Tables 2–5 shows the optimum neuron obtained for each of the countries investigated. In Table 2, optimized hidden neurons of 29 with MSE values of  $3.92 \times 10^{-21}$  was obtained for NARX neural network architecture using 13 delays. This resulted in a NARX model architecture of 5-29-1 representing the input layer, hidden neurons, and the output layer. This optimized NARX model architecture was subsequently obtained for modelling the prediction of CO<sub>2</sub> in Malaysia. Table 3 shows the variation of the hidden neurons for each iteration of the delay using the dataset for Thailand. Optimized hidden neurons of 19 with MSE value of  $4.15 \times 10^{-23}$  were obtained for the NARX neural network architecture using 13 delays resulting in an optimized network with the architecture of 5-19-1 denoting the input, hidden, and output layers, respectively. The subsequent modelling of the CO<sub>2</sub> prediction in Thailand was modelled using the optimized NARX model architecture. Tables 4 and 5 show the optimized neurons obtained using the datasets for Indonesia and the Philippines. An optimized 17 and 13 hidden neurons were obtained for the NARX neural network used for training the datasets for Indonesia, and the Philippines, respectively. This was achieved using 15 delays each for the optimized hidden neuron. Based on the optimized hidden neurons, NARX neural network model architectures of 5-17-1, and 5-13-1 were obtained for modeling the prediction of CO<sub>2</sub> emissions in Indonesia, and the Philippines, respectively. Besides the low MSE obtained, the suitability of the four optimized NARX models as robust predictive techniques were further ascertained from the high values of the R and R<sup>2</sup> which are greater than 0.9 as shown in Tables 2–5. The optimized architecture of the NARX models used for the predictive modelling of the CO<sub>2</sub> emissions in Malaysia, Thailand, Indonesia and the Philippines is generally represented in Figure 3 while the detailed architectures are depicted in Table 6. The optimized NARX models consist of the five input nodes, the hidden layers (which is made up of the optimized hidden neurons and delays) and the output node. The validation of each of the optimized NARX model is depicted in Figure 4. The best validation performance with MSE values of  $6.93 \times 10^{-4}$ ,  $9.26 \times 10^{-4}$ ,  $2.03 \times 10^{-3}$ , and  $7.99 \times 10^{-4}$  was obtained at the epoch of 6, 2, 7, and 11, respectively for Malaysia, Thailand, Indonesia and Philippines (Figure 4a–d). High epoch values indicate that it takes longer iterations for the best performance to be validated. Zounemat-Kermani et al. [38] have reported optimized NARX model architectures of 10-12-1, 10-10-1, 8-9-1, and 6-8-1 for modelling the prediction of gaseous emissions within the influent chamber of four different wastewater treatment plant. The variation in the NARX model architectures could be attributed to the nature of the input variables, the datasets and the non-linear relationship between the input and the output variables.

**Table 2.** Optimized hidden neuron obtained using data for Malaysia.

Model Architecture	Delay	Hidden Neurons	R	R <sup>2</sup>	MSE
5-25-1	1	25	0.974	0.949	$4.54 \times 10^{-4}$
5-27-1	3	27	0.996	0.992	$8.12 \times 10^{-5}$
5-29-1	5	29	0.998	0.996	$1.15 \times 10^{-4}$
5-9-1	7	9	0.999	0.998	$1.28 \times 10^{-5}$
5-15-1	9	15	0.998	0.996	$4.16 \times 10^{-5}$
5-7-1	11	7	0.999	0.998	$2.15 \times 10^{-20}$
5-29-1	13	29	0.999	0.998	$3.92 \times 10^{-21}$
5-7-1	15	7	0.999	0.998	$8.34 \times 10^{-17}$

**Table 3.** Optimized hidden neuron obtained using data for Thailand.

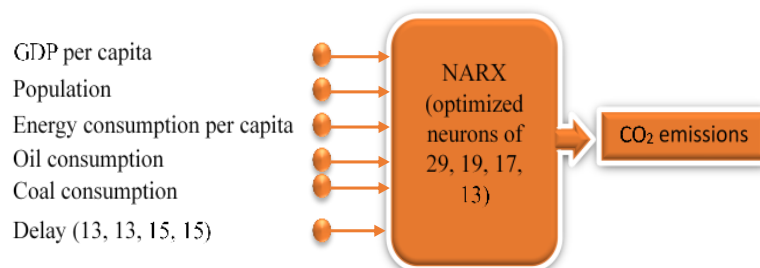
Model Architecture	Delay	Hidden Neurons	R	R <sup>2</sup>	MSE
5-29-1	1	29	0.987	0.974	$1.98 \times 10^{-4}$
5-19-1	3	19	0.999	0.998	$3.72 \times 10^{-10}$
5-23-1	5	23	0.999	0.998	$6.32 \times 10^{-19}$
5-11-1	7	11	0.999	0.998	$1.51 \times 10^{-8}$
5-25-1	9	25	0.999	0.998	$7.21 \times 10^{-6}$
5-25-1	11	25	0.999	0.998	$6.86 \times 10^{-21}$
5-19-1	13	19	0.999	0.998	$4.15 \times 10^{-23}$
5-5-1	15	5	0.999	0.998	$9.18 \times 10^{-19}$

**Table 4.** Optimized hidden neuron obtained using data for Indonesia.

Model Architecture	Delay	Hidden Neurons	R	R <sup>2</sup>	MSE
5-29-1	1	29	0.984	0.968	$4.37 \times 10^{-4}$
5-21-1	3	21	0.999	0.998	$7.18 \times 10^{-6}$
5-29-1	5	29	0.999	0.998	$1.75 \times 10^{-17}$
5-29-1	7	29	0.999	0.998	$1.25 \times 10^{-21}$
5-19-1	9	19	0.999	0.998	$1.36 \times 10^{-13}$
5-23-1	11	23	0.999	0.998	$1.83 \times 10^{-11}$
5-25-1	13	25	0.999	0.998	$5.35 \times 10^{-8}$
5-17-1	15	17	0.999	0.998	$2.02 \times 10^{-19}$

**Table 5.** Optimized hidden neuron obtained using data for Philippines.

Model Architecture	Delay	Hidden Neurons	R	R <sup>2</sup>	MSE
5-23-1	1	23	0.992	0.984	$7.05 \times 10^{-5}$
5-9-1	3	9	0.999	0.998	$2.40 \times 10^{-8}$
5-17-1	5	17	0.999	0.998	$4.99 \times 10^{-6}$
5-11-1	7	11	0.999	0.998	$2.94 \times 10^{-13}$
5-25-1	9	25	0.999	0.998	$6.97 \times 10^{-19}$
5-21-1	11	21	0.999	0.998	$2.11 \times 10^{-17}$
5-29-1	13	29	0.999	0.998	$8.82 \times 10^{-20}$
5-13-1	15	13	0.999	0.998	$1.32 \times 10^{-20}$

**Figure 3.** General representation of the optimized architecture for the NARX model used for prediction of CO<sub>2</sub> emissions in Malaysia, Thailand, Indonesia, and Philippines.**Table 6.** Details of the optimized NARX architecture used for the modeling.

	Malaysia	Thailand	Indonesia	Philippines
Input units	5	5	5	5
Optimized hidden neurons	13	19	17	13
Optimized delay	13	13	15	15
Output units	1	1	1	1

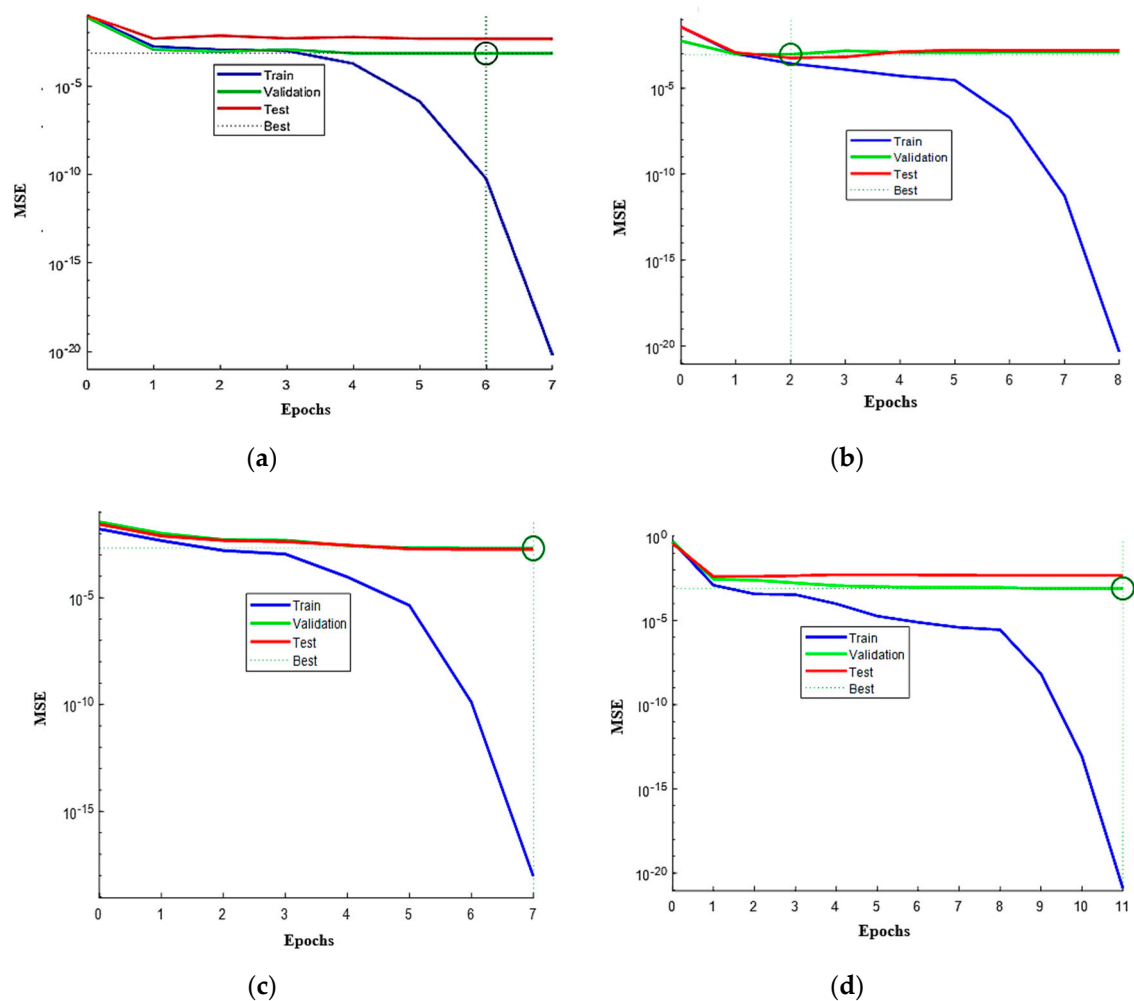


**Figure 4.** The validation performance of the optimized neuron at various epoch for (a) Malaysia; (b) Thailand; (c) Indonesia; and (d) the Philippines.

### 3.2. Performance Evaluation of the Optimized NARX Model

The performance of the optimized NARX models based on their predictability is depicted in Figure 5. It is obvious from the dispersion plots in Figure 5a–d that the actual values of the CO<sub>2</sub> emissions from Malaysia, Thailand, Indonesia, and the Philippines are in proximity with those predicted by the NARX models. The actual values of the CO<sub>2</sub> emissions are consistent with the predicted with high  $R^2 > 0.9$ . This can further be confirmed by the residuals shown in Figure 6. The residual range of  $-0.0005$  to  $+0.0094$  obtained for the predicted CO<sub>2</sub> emissions in the four ASEAN countries signifies that the NARX models possessed the capability to predict with minimal residuals. Besides very low MSE values (Tables 2–5) obtained for the optimized NARX model architecture is evidence of its robustness as a predictive modelling tool. The training, validation and testing of the datasets using the optimized NARX models are depicted in Figure 7. In each stage of the training, validation, and testing, the actual and the predicted CO<sub>2</sub> emissions of the four ASEAN countries understudied were obtained with minimized errors. The autocorrelation analyses of the NARX models used for the prediction of CO<sub>2</sub> emissions in the four ASEAN countries investigated are in Figure 8a–d. Most of the prediction errors are within the 95% confidence limits, which is an indication of the reliability of the estimations of the weight, bias and the network parameters [39]. The robustness of the NARX models employed in this study for the prediction of CO<sub>2</sub> emissions in four ASEAN countries is consistent with that reported by several authors reported in Literature and summarized in Table 7. Alcan et al. [40] for the prediction of NO<sub>x</sub> emissions from diesel engines. Using eight different input variables, the authors employed an



optimized NARX model architecture predictive modelling of NO<sub>x</sub> emissions. The findings revealed that the optimized NARX model architecture predicted the NO<sub>x</sub> emissions with a high degree of accuracy. Similarly, the work of Xu et al. [17] also confirms the applicability of NARX as a predictive modeling tool. The authors employed an optimized NARX model for the prediction of CO<sub>2</sub> emission in China using input variables which include gross economic output, urbanization, industrialization, urbanization, economic structure, total population, energy consumption and energy productivity. The findings revealed that the NARX model presented a more accurate prediction of CO<sub>2</sub> emissions in China compared to backpropagation neural networks and linear regression models. In a comparative study between NARX models and support vector machine for prediction of energy consumption in non-residential buildings, Koschwitz et al. [41] reported that NARX models displayed a better prediction of the energy consumption in the non-commercial buildings compared to support vector machine model. One major advantage of the NARX neural networks over the other modelling techniques is the ability to employed historical time series data for predictive modelling. Similarly, a multilayer perceptron type of Neural Network has been reported to accurately predict CO<sub>2</sub> absorption and solubility with low MSE values. [42,43].

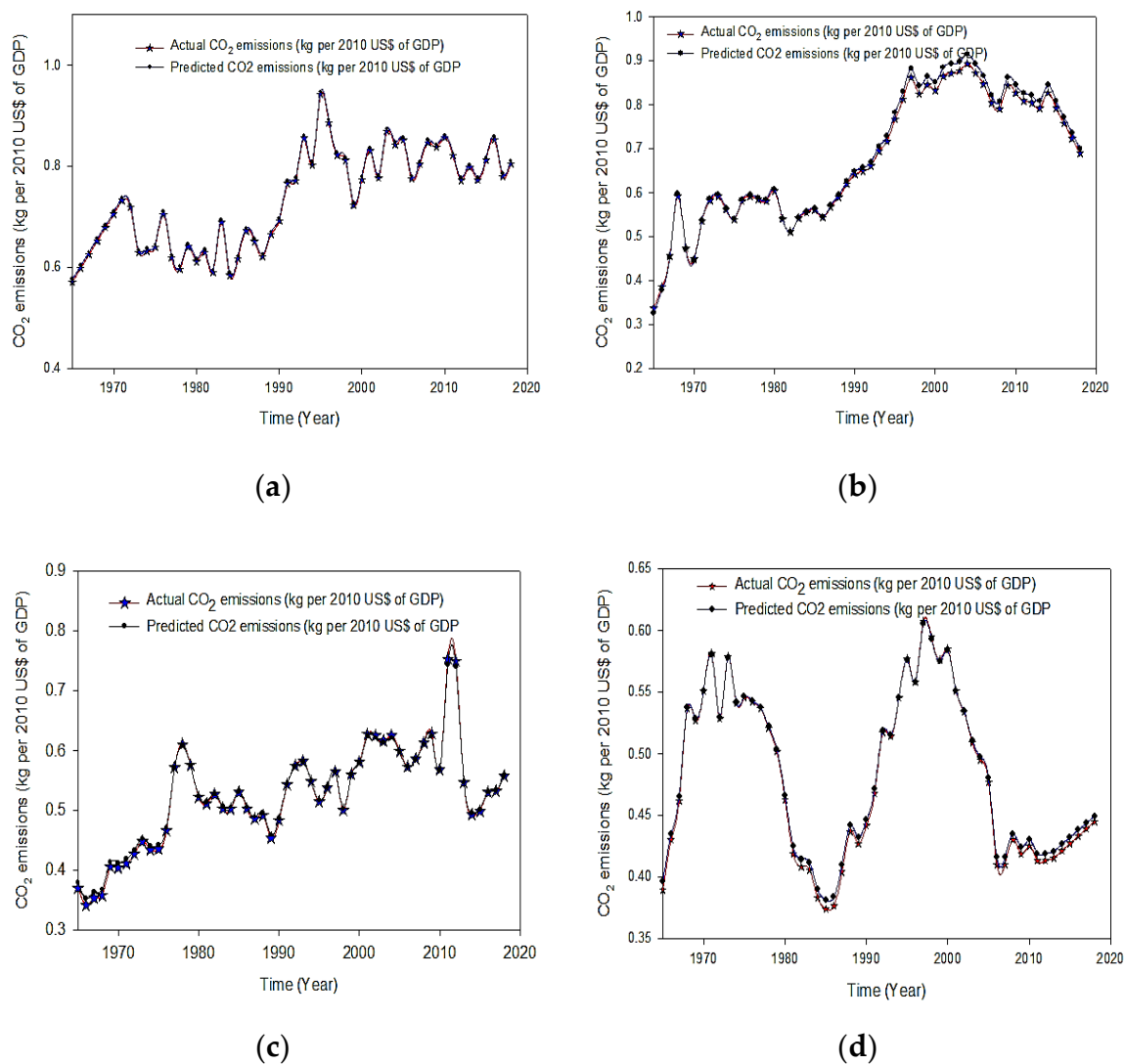


**Figure 5.** Dispersion plot showing the actual and predicted CO<sub>2</sub> emissions from (a) Malaysia, (b) Thailand, (c) Indonesia, (d) Philippines.

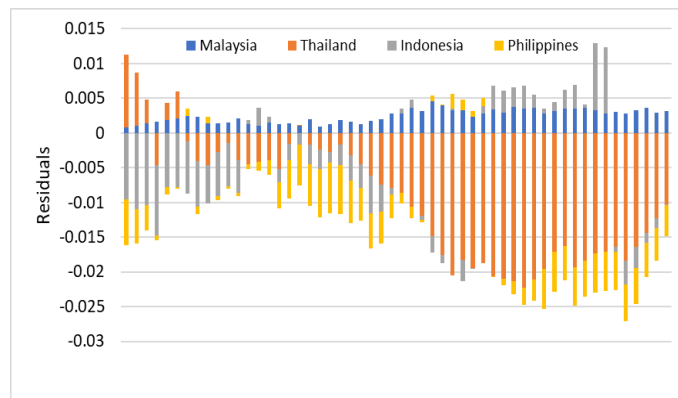


Figure 6. Residuals obtained from the NARX model prediction of CO<sub>2</sub> emissions.

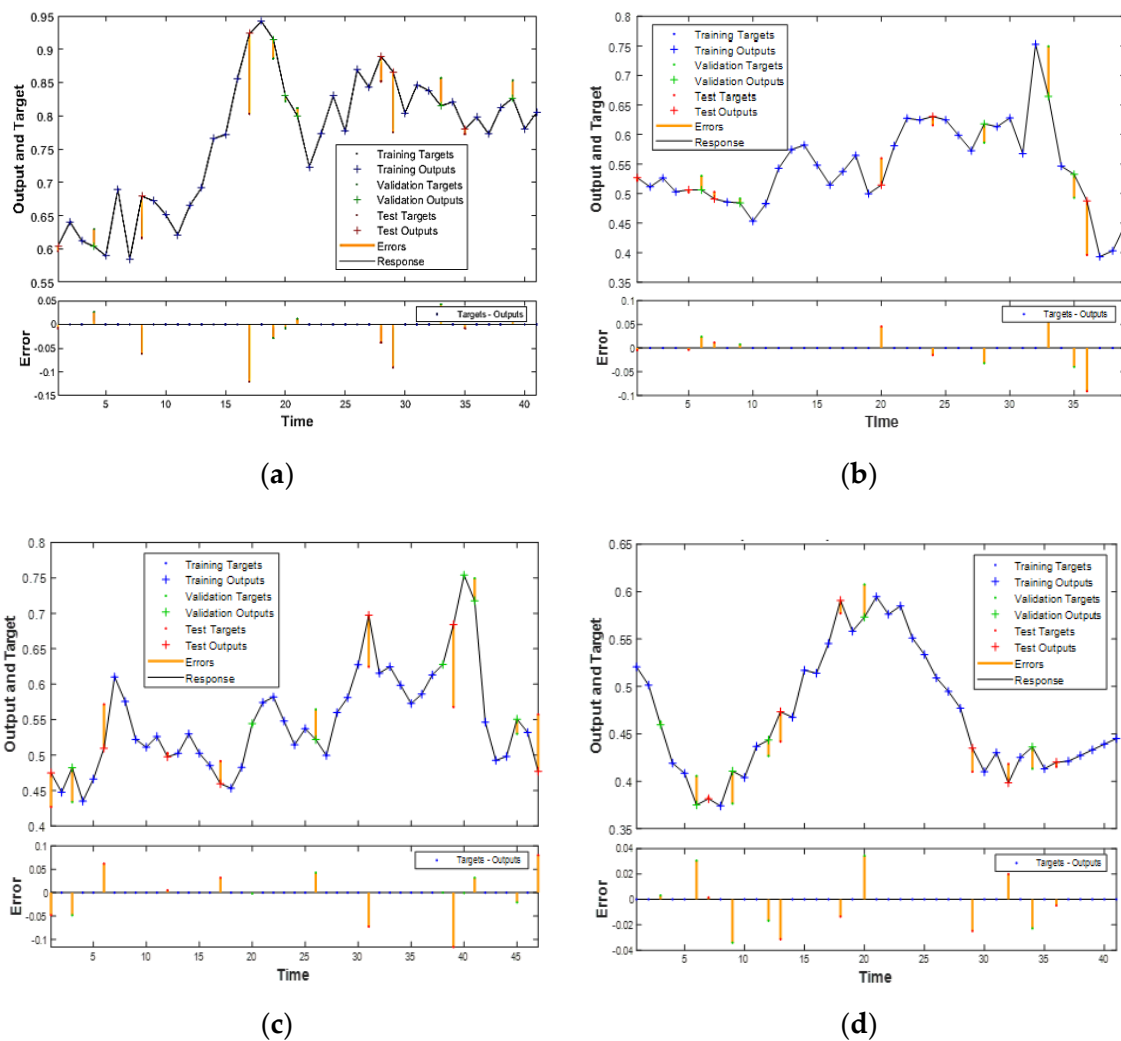
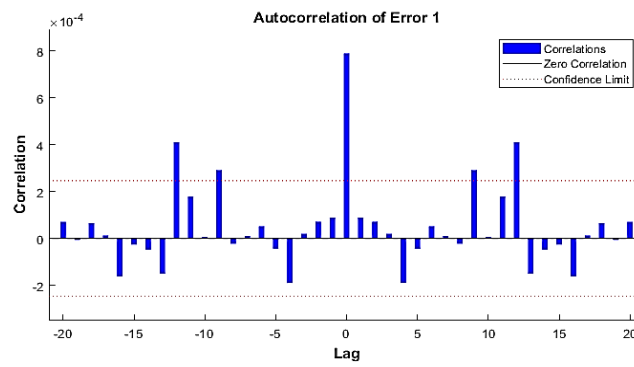
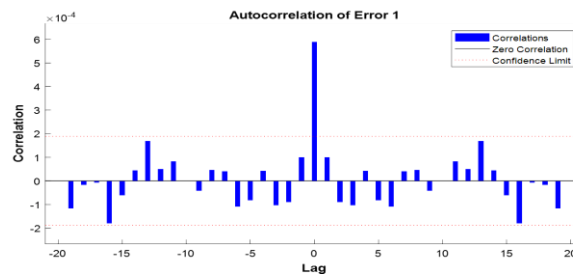


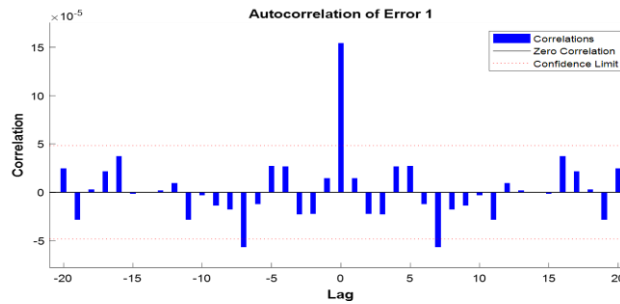
Figure 7. Comparison between the training, validation and testing responses of the NARX model. (a) Malaysia (b) Thailand, (c) Indonesia, (d) Philippines.



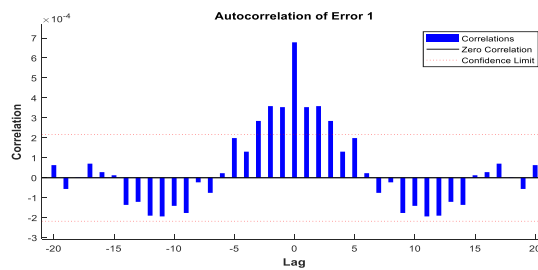
(a)



(b)



(c)



(d)

**Figure 8.** Autocorrelation analysis for the prediction of CO<sub>2</sub> emissions in (a) Malaysia, (b) Thailand, (c) Indonesia, (d) the Philippines.

**Table 7.** Comparison of the present work with literature.

Reference	Modelling Techniques	Objectives	Input Variables	Measurement of Accuracy	Conclusions
This work	NARX neural network	Predictive modelling of CO <sub>2</sub> emissions in four ASEAN countries	Energy consumption per capita, GDP per capita, population, oil consumption, coal consumption	MSE values of $6.93 \times 10^{-4}$ , $9.26 \times 10^{-4}$ , $2.03 \times 10^{-3}$ , and $7.99 \times 10^{-4}$ obtained for CO <sub>2</sub> emissions in Malaysia, Thailand, Indonesia, and the Philippines	The optimized NARX models efficiently predicted CO <sub>2</sub> emissions in the four ASEAN countries with coal consumptions having the highest level of importance. The optimized NARX model architecture predicted the NOx emissions with high degree of accuracy
Alcan et al. [40]	NARX neural network	Predictive modelling of NOx emissions from diesel engines	Engine speed, Manifold Absolute Pressure, Mass Air Flow, rail pressure, main and pilot injection fuel quantities, Main and pilot start of injections	Not reported	Economic scale, secondary sector (manufacturing and construction), coal consumption, industrialization, and energy productivity significantly influenced CO <sub>2</sub> emissions
Xu et al. [17]	NARX neural network	Predict CO <sub>2</sub> emission in China	GDP, total population, industrialization, urbanization, secondary sector, tertiary sector, total energy consumption, coal consumption, non-fossil consumption, energy productivity, investment in environment governance	RMSE = 0.0311	NARX models displayed a better prediction of the energy consumption in the non-commercial buildings compared to support vector machine
Koschwitz et al. [41]	NARX neural network and Support Vector Machine	Prediction of energy consumption in commercial building	dew point temperature, mean wind direction, mean wind velocity, outdoor temperature, precipitation intensity, precipitation quantity, relative humidity, school holiday time, working time schedule	MSE = 2.35–2.89	The findings revealed that the ANN models predicted CO <sub>2</sub> absorption was in proximity with the observed.
Pakzad et al. [42]	Multilayer Perceptron Neural Network	Modelling the CO <sub>2</sub> absorption	CO <sub>2</sub> partial pressure, temperature, AMP concentration, and MeOH concentration	Average absolute relative deviation (AARD%) = 1.95	The solubility of CO <sub>2</sub> in the mixed aqueous solution was accurately predicted by the Neural Network.
Hamzehie et al. [43]	Multilayer Perceptron Neural Network	Modelling the CO <sub>2</sub> solubility	Temperature, pressure, overall concentration, apparent molecular weight of the mixture.	MSE = $2.300 \times 10^{-4}$	

### 3.3. Sensitivity Analysis to Determine the Level of Importance of the Input Variables

The level of importance of the five variables namely GDP per capita, Population, Energy consumption per capita, coal consumption, and oil consumption are depicted in Figure 9. As shown in Figure 9a–d, the five variables have a significant level of importance on the CO<sub>2</sub> emissions in Malaysia, Thailand, Indonesia, and Thailand based on the sensitivity analyses. This is evidence from the values of the normalized importance which is greater than 50% for each of the variables. However, coal consumption with 100% normalized importance can be said to have the most significant influence on CO<sub>2</sub> emissions in Malaysia, Thailand, Indonesia, and the Philippines. According to the recent report by the International Energy Agency, Coal consumption used for electricity generation in the four ASEAN countries has been on the increase in the last decade [5]. For instance, coal consumption increased from 19.312 TOE December 2017 to 21.122 TOE in December 2018. Based on the Energy Commission Malaysia 2017 report, over 90% of electricity, generated in Peninsular Malaysia was from fossil fuel in which coal accounted for about 50% [44]. Similarly, coal consumption used for electricity generation in Thailand has also increased over the years [45]. Most of the electricity generated in Thailand are from fossil fuel, such as coal, natural gas and fuel oil [46]. The consumption of coal for electricity generation has also increased in Indonesia over the years [5]. Studies have shown that coal consumptions in Indonesia is expected to rise up to 157 million tons by 2027 thereby increasing the share of electricity generation from coal by 33.6% [47]. Hence, upwards in the amount of CO<sub>2</sub> emissions in Indonesia is also expected if there no commitment to diversify the electricity generation mix. In the Philippines, 70% of electricity generation is from fossil fuel mainly natural gas and coal out of which coal accounted for 42.8% as of 2018 [48]. There has been an annual increase in coal consumptions over the year which directly translated to an increase in CO<sub>2</sub> emissions. The causal relationship between coal consumption, CO<sub>2</sub> emission and economic growth has been reported by Al-Mulali and Che Sab [49]. The study which investigated ten countries revealed that coal consumption and CO<sub>2</sub> emissions have a short-run positive bidirectional relationship. This implies that an increase in coal consumption directly translated into more CO<sub>2</sub> emissions. Also, in conformity with these study authors such as Chang (2010) [50] and Chandran Govindaraju and Tang [28] have also reported the direct relationship between coal consumption and CO<sub>2</sub> emissions in China. Besides the significant influence of coal consumption on CO<sub>2</sub> emissions, other factors such as oil consumptions, energy consumption per capita, population, and GDP per capita has been reported to have various level of relationship with CO<sub>2</sub> emissions. Apergis and Payne [51,52], Ozturk and Acaravci [26] and Chang [50] reported that GDP and CO<sub>2</sub> emissions in six America countries and China have short-run unidirectional relationship. Also, Al-mulali et al. (2013) [53], Chandran Govindaraju and Tang [28], Saboori and Sulaiman [54] also reported a unidirectional relationship between energy consumption and CO<sub>2</sub> emissions in NEBA and five ASEAN countries. However, the modelling techniques did not capture the level of importance of these variables on the CO<sub>2</sub> emissions which we have reported in this study.

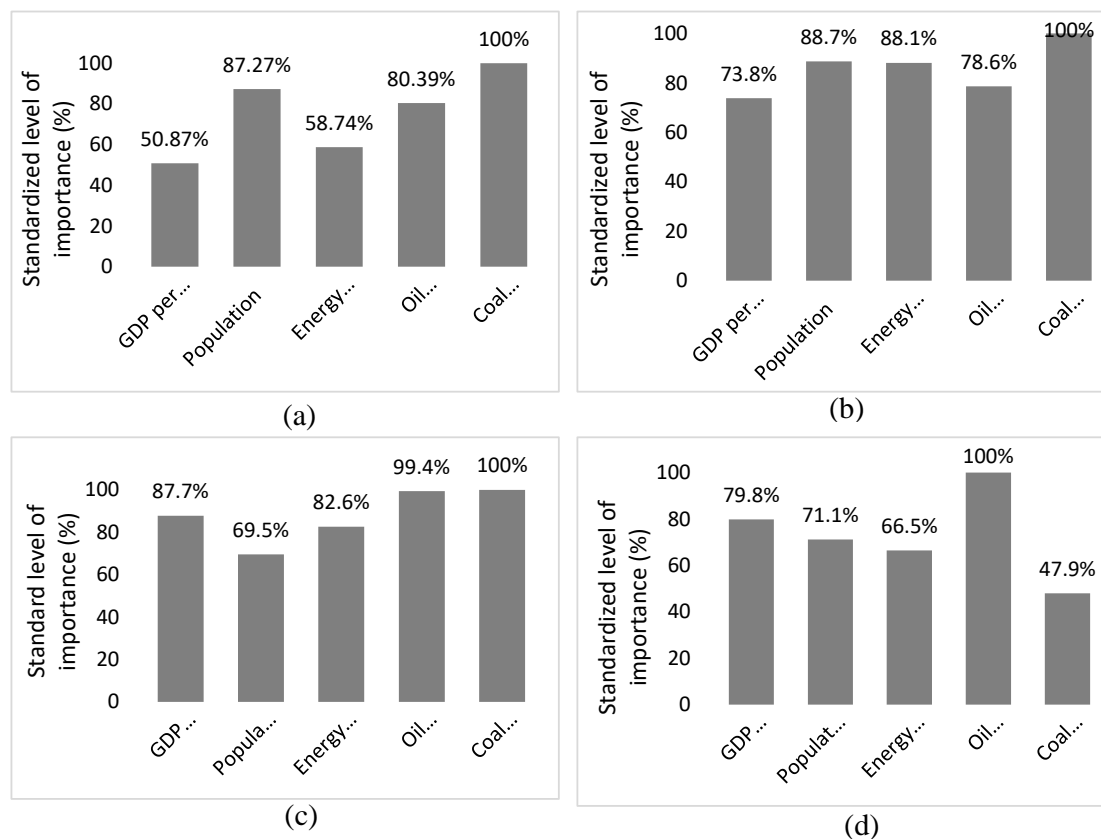


**Figure 9.** The level of importance of the input variables on the predicted CO<sub>2</sub> emissions in (a) Malaysia, (b) Thailand, (c) Indonesia, (d) Philippines.

#### 4. Conclusions and Policy Implications

This study demonstrates the application of a non-linear autoregressive exogenous neural network for modelling the prediction of CO<sub>2</sub> emissions in Malaysia, Thailand, Indonesia, and the Philippines. Based on the non-linear relationships between the CO<sub>2</sub> emissions and the input variables (energy and economic indicators), fifteen NARX model architectures were developed and trained using historical data obtained for the four ASEAN countries. Among the various NARX model trained, optimized configurations of 5-29-1, 5-19-1, 5-17-1, 5-13-1 were obtained using datasets for Malaysia, Thailand, Indonesia, and the Philippines, respectively. Robust predictions of CO<sub>2</sub> emissions in Malaysia, Thailand, Indonesia, and the Philippines were achieved using the optimized NARX model configurations. The predicted CO<sub>2</sub> emissions in the four ASEAN countries were in close agreement with the actual values from the historical data, as indicated by the high values of R<sup>2</sup>. The findings also show that the NARX models have high predictability with minimal residual and MSE due to its excellent learning ability, rapid convergence, and superior generalization. The level of importance analyses of the various factors revealed that the economic and energy indicators significantly influenced CO<sub>2</sub> emissions in the four ASEAN countries. Nevertheless, coal consumption displayed the highest level of importance on the CO<sub>2</sub> emissions in the four ASEAN countries. This calls for more commitment by the government and stakeholders in each of the four ASEAN countries for more stringent legislation and policies on the modalities to drastically reduce CO<sub>2</sub> emissions. Although, the governments of each of the four countries investigated have made various commitments to reduce energy-related CO<sub>2</sub> emissions. These include the mandatory use of smart street lighting systems and sustainable urban transport policies in Indonesia; the national biofuel policy, national renewable energy policy and the low carbon cities framework in Malaysia; the National Renewable Energy program in the Philippines; Climate Change Master plan in Thailand. However, more commitment is needed to reduce the CO<sub>2</sub> emissions in each of the four countries investigated. Governments of the four ASEAN countries should

give it a serious thought of domesticating the climate-neutral now policy proposed by the United Nation Climate Change which entails the measurements of the GHGs emissions, proposed action plans to reduce the GHGs emissions as much as possible, and the implementation of carbon credit, which involve compensating the GHGs emissions that cannot be avoided. Moreover, the ongoing efforts by the four countries in incorporating renewable energy as part of the primary energy mix should be intensified. The regional efforts should be strengthened to address the issues of CO<sub>2</sub> emissions in the ASEAN region. Considering the peculiarity of each country, collective policies targeting the reduction of CO<sub>2</sub> emissions could be formulated and each member committed to implementation. Based on the level of importance analysis in this study, direct target and strategies on the gradual replacement of coal as the main sources of energy in ASEAN countries should be put in place. Although, the NARX model used in this study has been demonstrated to be robust in predicting the CO<sub>2</sub> emissions in the four ASEAN countries investigated, the findings cannot be generalized and adapted for other ASEAN countries due to the uniqueness of each country's data. However, the NARX model could also be employed in a broader perspective by incorporating more data from other ASEAN countries. This could provide a robust CO<sub>2</sub> emission prediction for the whole ASEAN region and hence provide opportunity for a regional effort to develop modalities for reduction of CO<sub>2</sub> emissions in the region.

**Author Contributions:** S.I.M. and B.V.A. conceptualized the idea. F.O.A., B.V.A. and N.M. wrote the draft manuscript. SIM reviewed the draft manuscript for technicality. S.I.M. acquired the funding for the research. All authors have read and agreed to the published version of the manuscript.

**Funding:** This research and the APC was funded by Universiti Tenaga Nasional by grant number BOLD2025 (10436494/B2019141).

**Acknowledgments:** B.V.A., S.I.M., and S.M. acknowledge the financial support of Universiti Tenaga Nasional, Malaysia.

**Conflicts of Interest:** The authors declare that the research was conducted in the absence of any commercial or financial relationships that could be construed as a potential conflict of interest.

## Abbreviations

ASEAN	Association of Southeast Asian Nations
ARIMA	Auto-Regressive Integrated Moving Average
ARDL	Autoregressive Distributive Lag
CO <sub>2</sub>	Carbon dioxide
EKC	Environmental Kuznets Curve
FDI	Foreign Direct Investment
MSE	Mean Square Error
NARX	Non-linear Autoregressive neural network with Exogenous input
MAPE	Mean Absolute Percentage Error
TOE	Tonne of Oil Equivalent

Appendix A

**Table A1.** Detail results of the optimization of the hidden neurons at varying delay using training data for Malaysia.

Number of Delay	1		3		5		7		9		11		13		15	
Hidden Neurons	MSE	R	MSE	R	MSE	R	MSE	R	MSE	R	MSE	R	MSE	R	MSE	R
1	$2.54 \times 10^{-3}$	0.871	$1.56 \times 10^{-3}$	0.907	$1.85 \times 10^{-3}$	0.899	$2.32 \times 10^{-3}$	0.882	$3.24 \times 10^{-3}$	0.813	$2.80 \times 10^{-3}$	0.844	$1.77 \times 10^{-3}$	0.818	$3.42 \times 10^{-3}$	0.892
3	$2.13 \times 10^{-3}$	0.892	$9.46 \times 10^{-4}$	0.939	$2.01 \times 10^{-3}$	0.900	$5.75 \times 10^{-3}$	0.641	$3.84 \times 10^{-3}$	0.791	$1.74 \times 10^{-3}$	0.912	$4.24 \times 10^{-4}$	0.979	$1.35 \times 10^{-3}$	0.936
5	$1.78 \times 10^{-3}$	0.914	$2.47 \times 10^{-4}$	0.875	$1.24 \times 10^{-3}$	0.921	$3.68 \times 10^{-4}$	0.978	$5.72 \times 10^{-3}$	0.905	$1.42 \times 10^{-3}$	0.942	$5.07 \times 10^{-3}$	0.878	$1.21 \times 10^{-2}$	0.516
7	$1.80 \times 10^{-3}$	0.896	$2.88 \times 10^{-3}$	0.881	$1.43 \times 10^{-3}$	0.917	$1.43 \times 10^{-3}$	0.953	$1.42 \times 10^{-4}$	0.994	$2.15 \times 10^{-20}$	1.00	$2.58 \times 10^{-3}$	0.941	$8.34 \times 10^{-17}$	0.999
9	$2.07 \times 10^{-3}$	0.909	$4.59 \times 10^{-3}$	0.810	$1.14 \times 10^{-3}$	0.924	$1.28 \times 10^{-5}$	0.999	$2.66 \times 10^{-3}$	0.989	$1.43 \times 10^{-3}$	0.964	$9.05 \times 10^{-4}$	0.958	$4.08 \times 10^{-3}$	0.897
11	$1.68 \times 10^{-3}$	0.912	$1.08 \times 10^{-3}$	0.932	$1.24 \times 10^{-3}$	0.928	$8.17 \times 10^{-4}$	0.961	$1.46 \times 10^{-3}$	0.964	$2.78 \times 10^{-5}$	0.998	$1.06 \times 10^{-4}$	0.995	$7.46 \times 10^{-5}$	0.996
13	$1.17 \times 10^{-3}$	0.931	$1.55 \times 10^{-3}$	0.901	$1.74 \times 10^{-4}$	0.991	$1.83 \times 10^{-4}$	0.92	$6.57 \times 10^{-5}$	0.998	$4.13 \times 10^{-4}$	0.979	$2.79 \times 10^{-3}$	0.9334	$2.05 \times 10^{-9}$	0.999
15	$1.75 \times 10^{-3}$	0.892	$1.22 \times 10^{-3}$	0.933	$1.05 \times 10^{-3}$	0.958	$8.39 \times 10^{-4}$	0.974	$4.16 \times 10^{-5}$	0.998	$8.37 \times 10^{-3}$	0.702	$2.51 \times 10^{-4}$	0.997	$2.08 \times 10^{-3}$	0.949
17	$5.59 \times 10^{-4}$	0.964	$2.47 \times 10^{-3}$	0.986	$2.03 \times 10^{-4}$	0.989	$1.63 \times 10^{-4}$	0.952	$1.32 \times 10^{-3}$	0.937	$3.16 \times 10^{-5}$	0.998	$1.32 \times 10^{-4}$	0.998	$3.71 \times 10^{-5}$	0.999
19	$1.08 \times 10^{-3}$	0.936	$4.36 \times 10^{-3}$	0.976	$1.22 \times 10^{-3}$	0.946	$6.96 \times 10^{-4}$	0.96	$8.69 \times 10^{-3}$	0.963	$4.20 \times 10^{-20}$	1.00	$8.27 \times 10^{-5}$	0.997	$1.32 \times 10^{-3}$	0.974
21	1.65	0.898	$1.10 \times 10^{-3}$	0.945	$3.46 \times 10^{-4}$	0.989	$1.45 \times 10^{-3}$	0.931	$1.55 \times 10^{-3}$	0.992	$2.54 \times 10^{-3}$	0.883	$8.38 \times 10^{-9}$	0.999	$4.24 \times 10^{-4}$	0.977
23	$2.38 \times 10^{-3}$	0.887	$7.88 \times 10^{-4}$	0.957	$8.78 \times 10^{-4}$	0.975	$3.25 \times 10^{-3}$	0.983	$3.15 \times 10^{-4}$	0.988	$3.37 \times 10^{-17}$	0.999	$3.25 \times 10^{-16}$	0.999	$7.37 \times 10^{-4}$	0.986
25	$4.54 \times 10^{-4}$	0.974	$1.24 \times 10^{-3}$	0.903	$3.28 \times 10^{-3}$	0.885	$7.19 \times 10^{-4}$	0.969	$1.17 \times 10^{-3}$	0.978	$2.99 \times 10^{-4}$	0.987	$4.41 \times 10^{-9}$	0.999	$5.86 \times 10^{-4}$	0.977
27	$9.17 \times 10^{-4}$	0.957	$8.12 \times 10^{-5}$	0.996	$8.48 \times 10^{-4}$	0.953	$2.35 \times 10^{-4}$	0.994	$1.03 \times 10^{-4}$	0.995	$1.11 \times 10^{-4}$	0.986	$3.63 \times 10^{-4}$	0.984	$1.61 \times 10^{-2}$	0.699
29	$1.37 \times 10^{-3}$	0.925	$8.71 \times 10^{-3}$	0.965	$1.15 \times 10^{-4}$	0.998	$4.28 \times 10^{-3}$	0.924	$4.84 \times 10^{-3}$	0.915	$2.09 \times 10^{-8}$	0.999	$3.92 \times 10^{-21}$	0.999	$2.16 \times 10^{-4}$	0.998

**Table A2.** Detail results of the optimization of the hidden neurons at varying delay using training data for Thailand.

Number of Delays	1		3		5		7		9		11		13		15	
Hidden Neuron	MSE	R	MSE	R	MSE	R	MSE	R	MSE	R	MSE	R	MSE	R	MSE	R
1	$2.3 \times 10^{-3}$	0.381	$7.07 \times 10^{-4}$	0.933	$7.37 \times 10^{-4}$	0.944	$8.96 \times 10^{-3}$	0.548	$7.69 \times 10^{-3}$	0.117	$1.44 \times 10^{-3}$	0.898	$1.12 \times 10^{-3}$	0.967	$2.4 \times 10^{-3}$	0.805
3	$1.31 \times 10^{-3}$	0.912	$5.52 \times 10^{-3}$	0.567	$2.49 \times 10^{-3}$	0.806	$2.23 \times 10^{-3}$	0.827	$2.77 \times 10^{-3}$	0.741	1.56	0.905	$3.69 \times 10^{-4}$	0.997	$8.2 \times 10^{-4}$	0.957
5	1.101	0.937	$8.00 \times 10^{-3}$	0.613	$1.93 \times 10^{-3}$	0.869	$1.30 \times 10^{-3}$	0.900	$2.55 \times 10^{-5}$	0.998	$2.85 \times 10^{-3}$	0.786	$1.44 \times 10^{-4}$	0.99	$9.2 \times 10^{-19}$	0.999
7	$8.14 \times 10^{-4}$	0.953	$9.76 \times 10^{-4}$	0.948	$1.5 \times 10^{-3}$	0.899	$1.14 \times 10^{-3}$	0.931	$1.21 \times 10^{-5}$	0.999	$7.27 \times 10^{-4}$	0.936	$4.06 \times 10^{-3}$	0.995	$8.8 \times 10^{-12}$	0.999
9	$2.37 \times 10^{-3}$	0.863	$4.19 \times 10^{-3}$	0.973	$1.65 \times 10^{-3}$	0.851	$1.59 \times 10^{-3}$	0.875	$1.77 \times 10^{-3}$	0.804	$8.56 \times 10^{-5}$	0.997	$7.53 \times 10^{-4}$	0.958	$6.2 \times 10^{-8}$	0.999
11	$3.64 \times 10^{-4}$	0.979	$1.48 \times 10^{-3}$	0.898	$1.86 \times 10^{-7}$	0.999	$1.51 \times 10^{-8}$	0.999	$9.25 \times 10^{-5}$	0.994	$1.87 \times 10^{-3}$	0.923	$4.19 \times 10^{-3}$	0.772	$5.9 \times 10^{-5}$	0.997
13	$7.88 \times 10^{-3}$	0.627	$1.04 \times 10^{-4}$	0.992	$5.19 \times 10^{-4}$	0.966	$5.02 \times 10^{-4}$	0.947	$1.81 \times 10^{-3}$	0.909	$5.88 \times 10^{-4}$	0.964	$7.93 \times 10^{-9}$	0.999	$4.7 \times 10^{-3}$	0.813
15	$1.88 \times 10^{-3}$	0.892	$1.71 \times 10^{-3}$	0.881	$4.86 \times 10^{-3}$	0.613	$1.05 \times 10^{-3}$	0.968	$8.54 \times 10^{-4}$	0.923	$3.02 \times 10^{-3}$	0.998	$1.14 \times 10^{-3}$	0.914	$2.5 \times 10^{-3}$	0.914
17	$8.71 \times 10^{-3}$	0.951	$6.62 \times 10^{-4}$	0.954	$5.56 \times 10^{-4}$	0.95	$3.94 \times 10^{-3}$	0.817	$5.30 \times 10^{-5}$	0.997	$1.11 \times 10^{-3}$	0.937	$5.08 \times 10^{-6}$	0.999	$6.9 \times 10^{-18}$	0.999
19	$5.13 \times 10^{-3}$	0.963	$3.7 \times 10^{-10}$	0.999	$9.38 \times 10^{-5}$	0.993	$2.86 \times 10^{-4}$	0.984	$8.52 \times 10^{-5}$	0.995	$6.90 \times 10^{-4}$	0.956	$4.2 \times 10^{-23}$	0.999	$1.9 \times 10^{-5}$	0.879
21	$8.86 \times 10^{-4}$	0.949	$2.75 \times 10^{-4}$	0.959	$3.03 \times 10^{-3}$	0.847	$2.45 \times 10^{-6}$	0.999	$4.44 \times 10^{-3}$	0.963	$8.09 \times 10^{-4}$	0.954	$5.54 \times 10^{-5}$	0.997	$7.9 \times 10^{-5}$	0.994
23	$3.26 \times 10^{-3}$	0.984	$5.54 \times 10^{-3}$	0.775	$6.32 \times 10^{-19}$	0.999	$1.32 \times 10^{-4}$	0.998	$1.52 \times 10^{-3}$	0.907	$4.58 \times 10^{-8}$	0.999	$1.21 \times 10^{-9}$	0.999	$3.1 \times 10^{-7}$	0.999
25	$2.62 \times 10^{-3}$	0.874	$8.83 \times 10^{-4}$	0.949	$7.36 \times 10^{-4}$	0.945	$4.36 \times 10^{-4}$	0.971	$7.21 \times 10^{-6}$	0.999	$6.86 \times 10^{-21}$	0.999	$8.92 \times 10^{-4}$	0.931	$9.5 \times 10^{-5}$	0.992
27	$2.53 \times 10^{-3}$	0.856	$2.81 \times 10^{-3}$	0.841	$4.28 \times 10^{-13}$	0.999	$1.52 \times 10^{-4}$	0.993	$1.11 \times 10^{-5}$	0.999	$6.12 \times 10^{-11}$	0.999	$1.08 \times 10^{-4}$	0.996	$1.7 \times 10^{-3}$	0.994
29	$1.98 \times 10^{-4}$	0.987	$7.06 \times 10^{-4}$	0.974	$6.58 \times 10^{-3}$	0.546	$2.45 \times 10^{-5}$	0.998	$1.84 \times 10^{-4}$	0.992	$9.78 \times 10^{-4}$	0.999	$2.72 \times 10^{-5}$	0.999	$2.4 \times 10^{-3}$	0.999



**Table A3.** Detail results of the optimization of the hidden neurons at varying delay using training data for Indonesia.

Delay	1		3		5		7		9		11		13		15	
Hidden Neuron	MSE	R	MSE	R	MSE	R	MSE	R	MSE	R	MSE	R	MSE	R	MSE	R
1	$2.71 \times 10^{-3}$	0.852	$2.75 \times 10^{-3}$	0.811	$6.84 \times 10^{-4}$	0.946	$1.47 \times 10^{-3}$	0.837	$2.14 \times 10^{-3}$	0.753	$6.96 \times 10^{-5}$	0.993	$2.14 \times 10^{-3}$	0.697	$1.25 \times 10^{-3}$	0.932
3	$9.91 \times 10^{-4}$	0.935	$8.39 \times 10^{-4}$	0.885	$5.21 \times 10^{-4}$	0.935	$8.73 \times 10^{-4}$	0.929	$3.44 \times 10^{-4}$	0.952	$7.33 \times 10^{-4}$	0.882	$1.82 \times 10^{-3}$	0.865	$8.37 \times 10^{-4}$	0.904
5	$2.17 \times 10^{-3}$	0.855	$4.34 \times 10^{-4}$	0.965	$1.74 \times 10^{-3}$	0.832	$2.85 \times 10^{-3}$	0.869	$1.18 \times 10^{-3}$	0.911	$3.98 \times 10^{-3}$	0.684	$6.76 \times 10^{-3}$	0.991	$5.15 \times 10^{-4}$	0.939
7	$1.52 \times 10^{-3}$	0.909	$1.71 \times 10^{-4}$	0.99	$1.12 \times 10^{-3}$	0.923	$3.44 \times 10^{-3}$	0.563	$1.28 \times 10^{-3}$	0.984	$2.59 \times 10^{-3}$	0.981	$1.17 \times 10^{-3}$	0.898	$4.89 \times 10^{-3}$	0.739
9	$2.07 \times 10^{-3}$	0.868	$1.54 \times 10^{-3}$	0.857	$5.68 \times 10^{-5}$	0.996	$3.46 \times 10^{-3}$	0.815	$1.19 \times 10^{-5}$	0.999	$4.81 \times 10^{-3}$	0.419	$9.86 \times 10^{-4}$	0.901	$2.54 \times 10^{-4}$	0.972
11	$1.44 \times 10^{-3}$	0.901	$8.28 \times 10^{-5}$	0.992	$2.09 \times 10^{-3}$	0.991	$9.12 \times 10^{-3}$	0.991	$8.07 \times 10^{-5}$	0.991	$9.27 \times 10^{-6}$	0.995	$7.8 \times 10^{-10}$	0.999	$6.69 \times 10^{-3}$	0.959
13	$1.50 \times 10^{-3}$	0.919	$3.23 \times 10^{-4}$	0.962	$1.08 \times 10^{-3}$	0.9326	$1.16 \times 10^{-3}$	0.931	$1.41 \times 10^{-3}$	0.831	$8.68 \times 10^{-4}$	0.86	$1.82 \times 10^{-4}$	0.965	$4.73 \times 10^{-5}$	0.998
15	$5.54 \times 10^{-4}$	0.951	$1.39 \times 10^{-4}$	0.989	$6.39 \times 10^{-6}$	0.999	$2.01 \times 10^{-3}$	0.891	$7.08 \times 10^{-5}$	0.993	$5.01 \times 10^{-3}$	0.97	$2.54 \times 10^{-3}$	0.902	$7.45 \times 10^{-3}$	0.995
17	$4.51 \times 10^{-3}$	0.571	$1.04 \times 10^{-3}$	0.911	$1.86 \times 10^{-4}$	0.986	$2.09 \times 10^{-6}$	0.999	$1.38 \times 10^{-3}$	0.922	$1.35 \times 10^{-3}$	0.804	$8.04 \times 10^{-7}$	0.999	$9.28 \times 10^{-5}$	0.994
19	$4.63 \times 10^{-3}$	0.847	$2.70 \times 10^{-4}$	0.985	$1.83 \times 10^{-3}$	0.945	$1.19 \times 10^{-3}$	0.89	$1.36 \times 10^{-13}$	0.999	$4.65 \times 10^{-3}$	0.407	$6.11 \times 10^{-4}$	0.953	$1.4 \times 10^{-14}$	0.999
21	$2.13 \times 10^{-3}$	0.812	$7.18 \times 10^{-6}$	0.999	$1.23 \times 10^{-4}$	0.991	$1.31 \times 10^{-3}$	0.864	$2.87 \times 10^{-4}$	0.963	$2.17 \times 10^{-3}$	0.734	$1.94 \times 10^{-3}$	0.867	$1.29 \times 10^{-3}$	0.996
23	$1.12 \times 10^{-3}$	0.938	$7.83 \times 10^{-4}$	0.947	$4.01 \times 10^{-4}$	0.9728	$1.98 \times 10^{-3}$	0.981	$1.06 \times 10^{-3}$	0.819	$1.8 \times 10^{-11}$	0.999	$5.14 \times 10^{-4}$	0.929	$9.79 \times 10^{-5}$	0.987
25	5.94	0.957	$6.06 \times 10^{-4}$	0.956	$8.70 \times 10^{-4}$	0.992	$3.03 \times 10^{-3}$	0.97	$3.35 \times 10^{-3}$	0.997	$3.86 \times 10^{-4}$	0.969	$5.35 \times 10^{-8}$	0.999	$1.75 \times 10^{-3}$	0.928
27	$1.75 \times 10^{-3}$	0.874	$6.69 \times 10^{-4}$	0.952	$1.57 \times 10^{-3}$	0.857	$1.83 \times 10^{-3}$	0.986	$1.41 \times 10^{-3}$	0.847	$2.46 \times 10^{-3}$	0.829	$2.32 \times 10^{-3}$	0.759	$2.12 \times 10^{-6}$	0.999
29	$4.37 \times 10^{-4}$	0.984	$2.05 \times 10^{-4}$	0.986	$1.75 \times 10^{-17}$	0.999	$1.25 \times 10^{-21}$	0.999	$5.82 \times 10^{-4}$	0.954	$3.05 \times 10^{-3}$	0.967	$3.02 \times 10^{-3}$	0.992	$2.0 \times 10^{-19}$	0.999

**Table A4.** Detail results of the optimization of the hidden neurons at varying delay using training data for Philippines.

Delay	1		3		5		7		9		11		13		15	
Hidden Neuron	MSE	R	MSE	R	MSE	R	MSE	R	MSE	R	MSE	R	MSE	R	MSE	R
1	$3.55 \times 10^{-4}$	0.955	$4.27 \times 10^{-4}$	0.955	$2.12 \times 10^{-3}$	0.978	$4.06 \times 10^{-3}$	0.966	$1.14 \times 10^{-6}$	0.999	$8.8 \times 10^{-5}$	0.992	$1.21 \times 10^{-4}$	0.985	$9.64 \times 10^{-5}$	0.989
3	$3.73 \times 10^{-4}$	0.96	$6.95 \times 10^{-4}$	0.937	$2.08 \times 10^{-3}$	0.981	$6.64 \times 10^{-3}$	0.937	$6.92 \times 10^{-5}$	0.992	$2.35 \times 10^{-4}$	0.973	$1.05 \times 10^{-4}$	0.995	$2.11 \times 10^{-3}$	0.976
5	$3.13 \times 10^{-4}$	0.967	$2.32 \times 10^{-4}$	0.973	$1.13 \times 10^{-3}$	0.904	$2.56 \times 10^{-4}$	0.907	$5.61 \times 10^{-5}$	0.994	$6.12 \times 10^{-4}$	0.992	$1.41 \times 10^{-19}$	0.999	$5.59 \times 10^{-5}$	0.995
7	$8.76 \times 10^{-4}$	0.914	$3.41 \times 10^{-4}$	0.969	$1.64 \times 10^{-4}$	0.987	$2.71 \times 10^{-4}$	0.973	$1.94 \times 10^{-4}$	0.979	$7.09 \times 10^{-5}$	0.994	$4.08 \times 10^{-11}$	0.999	$3.88 \times 10^{-5}$	0.996
9	$2.61 \times 10^{-4}$	0.973	$2.40 \times 10^{-8}$	0.999	$1.45 \times 10^{-3}$	0.906	$7.52 \times 10^{-5}$	0.993	$9.48 \times 10^{-5}$	0.993	$4.98 \times 10^{-4}$	0.957	$4.56 \times 10^{-6}$	0.999	$5.95 \times 10^{-5}$	0.994
11	$4.24 \times 10^{-4}$	0.948	$2.16 \times 10^{-4}$	0.977	$2.56 \times 10^{-4}$	0.981	$2.9 \times 10^{-13}$	0.999	$2.04 \times 10^{-4}$	0.983	$6.07 \times 10^{-5}$	0.995	$1.21 \times 10^{-4}$	0.992	$5.51 \times 10^{-4}$	0.969
13	$1.18 \times 10^{-4}$	0.979	$7.92 \times 10^{-5}$	0.991	$1.95 \times 10^{-5}$	0.998	$2.14 \times 10^{-5}$	0.998	$7.89 \times 10^{-5}$	0.993	$8.48 \times 10^{-5}$	0.992	$2.46 \times 10^{-4}$	0.978	$1.32 \times 10^{-20}$	0.999
15	$1.14 \times 10^{-3}$	0.827	$2.48 \times 10^{-5}$	0.997	$3.31 \times 10^{-4}$	0.975	$1.73 \times 10^{-4}$	0.985	$4.36 \times 10^{-5}$	0.995	$2.27 \times 10^{-5}$	0.998	$3.66 \times 10^{-5}$	0.996	$9.91 \times 10^{-8}$	0.999
17	$3.17 \times 10^{-4}$	0.966	$9.55 \times 10^{-4}$	0.989	$4.99 \times 10^{-6}$	0.999	$8.8 \times 10^{-10}$	0.999	$4.86 \times 10^{-5}$	0.996	$6.65 \times 10^{-5}$	0.994	$4.32 \times 10^{-5}$	0.997	$1.21 \times 10^{-5}$	0.999
19	$8.43 \times 10^{-5}$	0.989	$5.94 \times 10^{-5}$	0.993	$4.56 \times 10^{-5}$	0.996	$7.15 \times 10^{-4}$	0.936	$4.18 \times 10^{-10}$	0.999	$6.22 \times 10^{-9}$	0.999	$2.82 \times 10^{-5}$	0.998	$2.22 \times 10^{-4}$	0.979
21	$3.59 \times 10^{-4}$	0.966	$2.09 \times 10^{-4}$	0.981	$3.56 \times 10^{-4}$	0.974	$1.64 \times 10^{-3}$	0.908	$1.09 \times 10^{-6}$	0.999	$2.11 \times 10^{17}$	0.999	$3.42 \times 10^{-5}$	0.996	$1.49 \times 10^{-8}$	0.999
23	$7.05 \times 10^{-4}$	0.992	$1.47 \times 10^{-4}$	0.983	$1.81 \times 10^{-4}$	0.982	$1.45 \times 10^{-3}$	0.901	$1.62 \times 10^{-4}$	0.987	$6.85 \times 10^{-5}$	0.993	$8.38 \times 10^{-6}$	0.999	$5.22 \times 10^{-4}$	0.972
25	$2.38 \times 10^{-4}$	0.971	$1.76 \times 10^{-5}$	0.998	$5.59 \times 10^{-4}$	0.931	$7.29 \times 10^{-5}$	0.995	$6.97 \times 10^{-19}$	0.999	$2.23 \times 10^{-5}$	0.998	$3.45 \times 10^{-4}$	0.959	$2.89 \times 10^{-5}$	0.998
27	$5.80 \times 10^{-4}$	0.929	$4.94 \times 10^{-5}$	0.994	$1.26 \times 10^{-4}$	0.987	$7.90 \times 10^{-5}$	0.993	$2.61 \times 10^{-5}$	0.997	$4.36 \times 10^{17}$	0.999	$4.91 \times 10^{-14}$	0.999	$7.96 \times 10^{-6}$	0.999
29	$1.24 \times 10^{-4}$	0.988	$6.29 \times 10^{-5}$	0.994	$1.78 \times 10^{-4}$	0.981	$2.18 \times 10^{-4}$	0.976	$4.88 \times 10^{-4}$	0.935	$6.25 \times 10^{-7}$	0.999	$8.82 \times 10^{-20}$	0.999	$8.92 \times 10^{-6}$	0.999

## References

1. Wang, Y.; Chen, L.; Kubota, J. The relationship between urbanization, energy use and carbon emissions: Evidence from a panel of Association of Southeast Asian Nations (ASEAN) countries. *J. Clean. Prod.* **2016**, *112*, 1368–1374. [[CrossRef](#)]
2. Tongsopit, S.; Kittner, N.; Chang, Y.; Aksornkij, A.; Wangjiraniran, W. Energy security in ASEAN: A quantitative approach for sustainable energy policy. *Energy Policy* **2016**, *90*, 60–72. [[CrossRef](#)]
3. Shi, X. The future of ASEAN energy mix: A SWOT analysis. *Renew. Sustain. Energy Rev.* **2016**, *53*, 672–680. [[CrossRef](#)]
4. Silbergliitt, R.; Kimmel, S. Energy scenarios for Southeast Asia. *Technol. Forecast. Soc. Chang.* **2015**, *101*, 251–262. [[CrossRef](#)]
5. *International Energy Agency Southeast Asia Energy Outlook 2017*; Southeast Asia Energy Outlook: Paris, France, 2017.
6. Mensah, I.A.; Sun, M.; Gao, C.; Omari-Sasu, A.Y.; Zhu, D.; Ampimah, B.C.; Quarcoo, A. Analysis on the nexus of economic growth, fossil fuel energy consumption, CO<sub>2</sub> emissions and oil price in Africa based on a PMG panel ARDL approach. *J. Clean. Prod.* **2019**, *228*, 161–174. [[CrossRef](#)]
7. Mardani, A.; Štreimikienė, D.; Cavallaro, F.; Loganathan, N.; Khoshnoudi, M. Carbon dioxide (CO<sub>2</sub>) emissions and economic growth: A systematic review of two decades of research from 1995 to 2017. *Sci. Total Environ.* **2019**, *649*, 31–49. [[CrossRef](#)]
8. Kasman, A.; Duman, Y.S. CO<sub>2</sub> emissions, economic growth, energy consumption, trade and urbanization in new EU member and candidate countries: A panel data analysis. *Econ. Model.* **2015**, *44*, 97–103. [[CrossRef](#)]
9. Tzeremes, P. Time-varying causality between energy consumption, CO<sub>2</sub> emissions, and economic growth: Evidence from US states. *Environ. Sci. Pollut. Res.* **2017**, *25*, 6044–6060. [[CrossRef](#)]
10. Ozcan, B.; Tzeremes, P.G.; Tzeremes, N.G. Energy consumption, economic growth and environmental degradation in OECD countries. *Econ. Model.* **2020**, *84*, 203–213. [[CrossRef](#)]
11. Zhu, H.; Duan, L.; Guo, Y.; Yu, K. The effects of FDI, economic growth and energy consumption on carbon emissions in ASEAN-5: Evidence from panel quantile regression. *Econ. Model.* **2016**, *58*, 237–248. [[CrossRef](#)]
12. Heidari, H.; Katircioğlu, S.T.; Saeidpour, L. Economic growth, CO<sub>2</sub> emissions, and energy consumption in the five ASEAN countries. *Int. J. Electr. Power Energy Syst.* **2015**, *64*, 785–791. [[CrossRef](#)]
13. Salman, M.; Long, X.; Dauda, L.; Mensah, C.N.; Muhammad, S. Different impacts of export and import on carbon emissions across 7 ASEAN countries: A panel quantile regression approach. *Sci. Total Environ.* **2019**, *686*, 1019–1029. [[CrossRef](#)] [[PubMed](#)]
14. Nugraha, A.T.; Osman, N.H. CO<sub>2</sub> emissions, economic growth, energy consumption, and household expenditure for Indonesia: Evidence from cointegration and vector error correction model. *Int. J. Energy Econ. Policy* **2019**, *9*, 291–298. [[CrossRef](#)]
15. Fatima, S.; Ali, S.S.; Zia, S.S.; Hussain, E.; Fraz, T.R.; Khan, M.S. Forecasting Carbon Dioxide Emission of Asian Countries Using ARIMA and Simple Exponential Smoothing Models. *Int. J. Econ. Environ. Geol.* **2019**, *10*, 64–69. [[CrossRef](#)]
16. Hanif, I.; Raza, S.M.F.; Gago-De-Santos, P.; Abbas, Q. Fossil fuels, foreign direct investment, and economic growth have triggered CO<sub>2</sub> emissions in emerging Asian economies: Some empirical evidence. *Energy* **2019**, *171*, 493–501. [[CrossRef](#)]
17. Xu, G.; Schwarz, P.; Yang, H. Determining China's CO<sub>2</sub> emissions peak with a dynamic nonlinear artificial neural network approach and scenario analysis. *Energy Policy* **2019**, *128*, 752–762. [[CrossRef](#)]
18. Kahouli, B. The causality link between energy electricity consumption, CO<sub>2</sub> emissions, R&D stocks and economic growth in Mediterranean countries (MCs). *Energy* **2018**, *145*, 388–399. [[CrossRef](#)]
19. Marczjasz, G.; Uniejewski, B.; Weron, R. On the importance of the long-term seasonal component in day-ahead electricity price forecasting with NARX neural networks. *Int. J. Forecast.* **2019**, *35*, 1520–1532. [[CrossRef](#)]
20. Alsaffar, M.A.; Ayodele, B.V.; Mustapa, S.I. Scavenging carbon deposition on alumina supported cobalt catalyst during renewable hydrogen-rich syngas production by methane dry reforming using artificial intelligence modeling technique. *J. Clean. Prod.* **2020**, *247*, 119168. [[CrossRef](#)]
21. Yang, Z.; Zhao, Y. Energy consumption, carbon emissions, and economic growth in India: Evidence from directed acyclic graphs. *Econ. Model.* **2014**, *38*, 533–540. [[CrossRef](#)]

22. Omri, A.; Nguyen, D.K.; Rault, C. Causal interactions between CO<sub>2</sub> emissions, FDI, and economic growth: Evidence from dynamic simultaneous-equation models. *Econ. Model.* **2014**, *42*, 382–389. [[CrossRef](#)]
23. Feng, Y.; Chen, S.; Zhang, L. System dynamics modeling for urban energy consumption and CO<sub>2</sub> emissions: A case study of Beijing, China. *Ecol. Model.* **2013**, *252*, 44–52. [[CrossRef](#)]
24. Pao, H.-T.; Yu, H.-C.; Yang, Y.-H. Modeling the CO<sub>2</sub> emissions, energy use, and economic growth in Russia. *Energy* **2011**, *36*, 5094–5100. [[CrossRef](#)]
25. Alam, M.J.; Begum, I.A.; Buysse, J.; Rahman, S.; Van Huylenbroeck, G. Dynamic modeling of causal relationship between energy consumption, CO<sub>2</sub> emissions and economic growth in India. *Renew. Sustain. Energy Rev.* **2011**, *15*, 3243–3251. [[CrossRef](#)]
26. Maziarz, M. A review of the Granger-causality fallacy. *J. Philos. Econ. Reflect. Econ. Soc. Issues* **2015**, *8*, 86–105.
27. Liu, X.; Mao, G.; Ren, J.; Li, R.Y.M.; Guo, J.; Zhang, H.-L. How might China achieve its 2020 emissions target? A scenario analysis of energy consumption and CO<sub>2</sub> emissions using the system dynamics model. *J. Clean. Prod.* **2015**, *103*, 401–410. [[CrossRef](#)]
28. Govindaraju, V.C.; Tang, C.F. The dynamic links between CO<sub>2</sub> emissions, economic growth and coal consumption in China and India. *Appl. Energy* **2013**, *104*, 310–318. [[CrossRef](#)]
29. Hossain, M.A.; Ayodele, B.V.; Cheng, C.K.; Khan, M.R. Artificial neural network modeling of hydrogen-rich syngas production from methane dry reforming over novel Ni/CaFe<sub>2</sub>O<sub>4</sub> catalysts. *Int. J. Hydrog. Energy* **2016**, *41*, 11119–11130. [[CrossRef](#)]
30. Saghafi, M.; Ghofrani, M.B. Real-time estimation of break sizes during LOCA in nuclear power plants using NARX neural network. *Nucl. Eng. Technol.* **2019**, *51*, 702–708. [[CrossRef](#)]
31. Rahmani, A.; Deihimi, A. Reduction of harmonic monitors and estimation of voltage harmonics in distribution networks using wavelet analysis and NARX. *Electr. Power Syst. Res.* **2020**, *178*, 106046. [[CrossRef](#)]
32. Ezzeldin, R.; Hatata, A.Y. Application of NARX neural network model for discharge prediction through lateral orifices. *Alex. Eng. J.* **2018**, *57*, 2991–2998. [[CrossRef](#)]
33. Garson, G.D. Comparison of Neural Network Analysis of Social Science Data. *Soc. Sci. Comput. Rev.* **1991**, *9*, 399–434. [[CrossRef](#)]
34. Cheng, J.; Ji, Z.; Li, M.; Dai, J. Study of a noninvasive blood glucose detection model using the near-infrared light based on SA-NARX. *Biomed. Signal Process. Control* **2020**, *56*, 101694. [[CrossRef](#)]
35. Pazikadin, A.R.; Rifai, D.; Ali, K.; Malik, M.Z.; Abdalla, A.N.; Faraj, M.A. Solar irradiance measurement instrumentation and power solar generation forecasting based on Artificial Neural Networks (ANN): A review of five years research trend. *Sci. Total Environ.* **2020**, *715*, 136848. [[CrossRef](#)]
36. Giannopoulos, A.; Aider, J.-L. Prediction of the dynamics of a backward-facing step flow using focused time-delay neural networks and particle image velocimetry data-sets. *Int. J. Heat Fluid Flow* **2020**, *82*, 108533. [[CrossRef](#)]
37. Das, S.K.; Basudhar, P.K. Prediction of residual friction angle of clays using artificial neural network. *Eng. Geol.* **2008**, *100*, 142–145. [[CrossRef](#)]
38. Zounemat-Kermani, M.; Stephan, D.; Hinkelmann, R. Multivariate NARX neural network in prediction gaseous emissions within the influent chamber of wastewater treatment plants. *Atmos. Pollut. Res.* **2019**, *10*, 1812–1822. [[CrossRef](#)]
39. Oko, E.; Wang, M.; Zhang, J. Neural network approach for predicting drum pressure and level in coal-fired subcritical power plant. *Fuel* **2015**, *151*, 139–145. [[CrossRef](#)]
40. Alcan, G.; Unel, M.; Aran, V.; Yilmaz, M.; Gurel, C.; Koprubasi, K. Predicting NO<sub>x</sub> emissions in diesel engines via sigmoid NARX models using a new experiment design for combustion identification. *Measurements* **2019**, *137*, 71–81. [[CrossRef](#)]
41. Koschwitz, D.; Frisch, J.; Van Treeck, C. Data-driven heating and cooling load predictions for non-residential buildings based on support vector machine regression and NARX Recurrent Neural Network: A comparative study on district scale. *Energy* **2018**, *165*, 134–142. [[CrossRef](#)]
42. Pakzad, P.; Mofarahi, M.; Izadpanah, A.A.; Afkhamipour, M. Experimental data, thermodynamic and neural network modeling of CO<sub>2</sub> absorption capacity for 2-amino-2-methyl-1-propanol (AMP) + Methanol (MeOH) + H<sub>2</sub>O system. *J. Nat. Gas Sci. Eng.* **2020**, *73*, 103060. [[CrossRef](#)]
43. Hamzehie, M.; Mazinani, S.; Davardoost, F.; Mokhtare, A.; Najibi, H.; Van Der Bruggen, B.; Darvishmanesh, S. Developing a feed forward multilayer neural network model for prediction of CO<sub>2</sub> solubility in blended aqueous amine solutions. *J. Nat. Gas Sci. Eng.* **2014**, *21*, 19–25. [[CrossRef](#)]

44. Energy in Malaysia. *Toward a World-Class Energy Sector*; Suruhanjaya Tenaga: Putrajaya, Malaysia, 2017; Volume 12, pp. 1–45.
45. Kenney, W. *Energy Conservation in the Process Industries*; Elsevier: Amsterdam, The Netherlands, 1984; pp. 1–17.
46. *Gross Energy Generation and Purchase*; EGAT: Bangkok, Thailand, 2019.
47. *Handbook of Energy & Economic Statistics of Indonesia 2018*; Ministry of Energy and Mineral Resources, Republic of Indonesia: Jakarta, Indonesia, 2018.
48. *Philippines Power Statistics*; Department of Energy: Taguig, Philippines, 2019.
49. Al-Mulali, U.; Sab, C.N.B.C. Electricity consumption, CO<sub>2</sub> emission, and economic growth in the Middle East. *Energy Sources Part B Econ. Plan. Policy* **2018**, *13*, 257–263. [[CrossRef](#)]
50. Chang, C.-C. A multivariate causality test of carbon dioxide emissions, energy consumption and economic growth in China. *Appl. Energy* **2010**, *87*, 3533–3537. [[CrossRef](#)]
51. Apergis, N.; Payne, J.E. CO<sub>2</sub> emissions, energy usage, and output in Central America. *Energy Policy* **2009**, *37*, 3282–3286. [[CrossRef](#)]
52. Apergis, N.; Payne, J.E. The emissions, energy consumption, and growth nexus: Evidence from the commonwealth of independent states. *Energy Policy* **2010**, *38*, 650–655. [[CrossRef](#)]
53. Al-Mulali, U.; Fereidouni, H.G.; Lee, J.Y.; Sab, C.N.B.C. Exploring the relationship between urbanization, energy consumption, and CO<sub>2</sub> emission in MENA countries. *Renew. Sustain. Energy Rev.* **2013**, *23*, 107–112. [[CrossRef](#)]
54. Saboori, B.; Sulaiman, J. Environmental degradation, economic growth and energy consumption: Evidence of the environmental Kuznets curve in Malaysia. *Energy Policy* **2013**, *60*, 892–905. [[CrossRef](#)]

**Publisher’s Note:** MDPI stays neutral with regard to jurisdictional claims in published maps and institutional affiliations.



© 2020 by the authors. Licensee MDPI, Basel, Switzerland. This article is an open access article distributed under the terms and conditions of the Creative Commons Attribution (CC BY) license (<http://creativecommons.org/licenses/by/4.0/>).